Evidence for Coherent Collective Rydberg Excitation in the Strong Blockade Regime

Rolf Heidemann,[1,*] Ulrich Krohn,[1] Vera Bendkowsky,[1] Björn Butscher,[1] Robert Löw,[1] Luis Santos,[2] and Tilman Pfau[1,†]

[1]*5. Physikalisches Institut, Universität Stuttgart, Pfaffenwaldring 57, 70569 Stuttgart, Germany*

[2]*Institut für Theoretische Physik, Universität Hannover, Appelstraße 2, 30167 Hannover, Germany*

(Received 19 June 2007; published 16 October 2007)

We report on strong van der Waals blockade in two-photon Rydberg excitation of ultracold magnetically trapped ^{87}Rb atoms. The excitation dynamics was investigated for a large range of densities and laser intensities and shows a full saturation and a strong suppression with respect to single-atom behavior. The observed scaling of the initial increase with density and laser intensity provides evidence for coherent collective excitation. This coherent collective behavior, that was observed for up to several thousand atoms per blockade volume, is generic for all mesoscopic systems which are able to carry only one single quantum of excitation.

DOI: 10.1103/PhysRevLett.99.163601 PACS numbers: 42.50.Fx, 32.80.Qk, 32.80.Rm, 34.20.Cf

Early studies on atomic beams, where line broadening effects at high Rydberg densities were observed [1], triggered experiments on ultracold samples [2–11]. The atomic motion of the atoms during the lifetime of the Rydberg atoms can be neglected at these ultralow temperatures. Therefore this excited state of matter is known as frozen Rydberg gas. The interaction between Rydberg atoms leads to a blockade effect which has been proposed as a crucial ingredient for quantum gates, either using single neutral atoms [12] or mesoscopic samples [13]. This blockade effect has been studied in various experiments using laser cooled atoms [4–6]. Typically the interaction effect was studied by changing the density of Rydberg atoms or by changing the principal quantum number n of the excited Rydberg state. As the van der Waals interaction scales with n^{11} a reduction of the excitation rates was observed for increasing n. A related interaction, the resonant dipole-dipole interaction, has been investigated [3,8] by tuning an electric field. Many-body effects between few atoms due to this interaction have been spectroscopically resolved [2] and their dependence on dimensionality was studied [10]. Coherent excitation of noninteracting ultracold atoms into a Rydberg state has been achieved with the use of stimulated Raman adiabatic passage sequences [7,11] and has recently been observed in electromagnetically induced transparency spectra [14].

Collective behavior is expected in all mesoscopic systems carrying a single quantum of excitation only, like an exciton in a quantum dot or a dark state polariton excited by a single photon in an ensemble of N atoms [15]. In the latter the time scale for the coherent evolution of the mesoscopic ensemble speeds up by a $\sqrt{N}$ factor, which is an important factor for quantum repeaters enabling long-distance quantum communication [16]. Analogous collective effects as reported here are meanwhile also observed in the coupling of a BEC to the mode of a cavity [17].

Using the setup discussed in [18], a number of $N_g = 1.5 \times 10^7$ ^{87}Rb atoms are magnetically trapped in the $5S_{1/2}$, $F = 2$, $m_F = 2$ state at a temperature of 3.4 μK. This sample in a Ioffe-Pritchard-type trap has a Gaussian density distribution with a peak value $n_{g,0}$ of 8.2×10^{13} cm^{-3}. The excitation to the $43S_{1/2}$ Rydberg state is done with a two-photon transition via the $5P_{3/2}$ state. To avoid significant population in the intermediate state the light is blue detuned by $\Delta = 478$ MHz from the $5P_{3/2}$, $F = 3$ level. We excite a Rydberg-S state as it has only one repulsive branch in its molecular potential [see Fig. 1(a)], whereas higher l states typically have repulsive and attractive branches and are subject to enhanced ion formation. Resonant dipole-dipole interaction due to the dominating transition $43S + 43S \rightarrow 42P + 43P$ is negligible for this

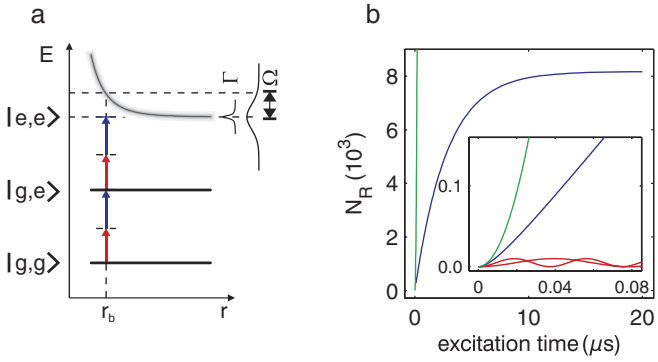

FIG. 1 (color). (a) Schematic view of molecular potential curves as a function of the relative coordinate r (the blue and red arrows symbolize the two-photon transition). The strong van der Waals interaction between the excited Rydberg states leads to a blockade effect for $|e, e\rangle$. Double excitation for distances smaller than the blockade radius r_b is strongly suppressed. For two atoms the blockade radius is either determined by the linewidth Γ or the power broadening Ω [see Eq. (2)]. (b) Shows a schematic of the Rydberg atom number N_R versus excitation time in an inhomogeneous sample. Many superatom oscillations (shown with 10 times exaggerated amplitudes in red) add up to an integrated saturation curve (blue). This curve falls behind the noninteracting case (shown for short times in green).

experiment [19]. The Rabi frequency Ω_1 for the $5S - 5P$ transition was determined by Autler-Townes splitting at higher intensities [20]. In the present experiment Ω_1 is varied from 2.0 to 9.7 MHz. A Rabi frequency Ω_2 for the upper transition of 21 MHz, which is estimated from our calculation of the dipole matrix element, results in a two-photon Rabi frequency $\Omega_0 = \Omega_1\Omega_2/(2\Delta)$ of up to 210 kHz. Since the waists of the Gaussian laser beams are large compared to the $1/e^2$ radius of the sample, the Rabi frequency is almost constant over the sample. The linewidth of excitation Γ was measured to be smaller than 1.5 MHz on the millisecond time scale and 130 kHz on the microsecond time scale. The latter was measured in a similar way as reported in Ref. [21] by an echo-type experiment where the excitation dynamics could be reversed. To reduce interaction effects in this measurement, an exceptionally low density was used.

The excitation dynamics are investigated, by switching the excitation lasers on for a time τ, that is varied between 100 ns and 20 μs and which is shorter than the 100 μs lifetime of the $43S$ state [18,22]. Although the thermal motion of the ground state atoms is frozen out on the time scale of the excitation, attractive interaction between the Rydberg atoms can lead to collisions and ionization within this time scale [19,23]. To avoid all effects of ions and electrons on the Rydberg atoms we chose a Rydberg state with repulsive van der Waals interaction ($C_6 = -1.7 \times 10^{19}$ a.u. [24]) and applied an electric field of 200 V/m strength during the excitation. This field suppresses enhanced ionization by means of trapped electrons [25], which would otherwise limit the lifetime [26]. The excitation line shows a density dependent blueshift in the presence of this field and a redshift without the field. This blueshift is a clear evidence for repulsive interaction whereas we attribute the redshift to a Stark shift induced by the electric field of charged particles. The tuning of the lasers to the two-photon resonance was determined from an excitation spectrum with very low laser power. This produced low Rydberg densities at which neither line shift nor broadening due to interactions were observed. Directly after the excitation pulse the excited Rydberg atoms are field ionized and the ions detected with a calibrated microchannel plate (MCP) detector.

In addition to the variation of excitation times, the two-photon Rabi frequency Ω_0 as well as the peak density $n_{g,0}$ of the ground state atoms were varied. This was done by changing the power of the 780 nm excitation laser and by transferring up to 97% of the atoms with a 6.8 GHz microwave Landau-Zener sweep of variable duration to the untrapped $5S_{1/2}$, $F = 1$, $m_F = 1$ state. The peak density was changed by this technique with virtually no change in temperature and shape of the density distribution. Every excitation and detection of the field-ionized Rydberg atoms is followed by a 20 ms time-of-flight of the remaining atoms. The atom number of remaining ground state atoms is obtained from an absorption image. The density distribution is calculated from this number and the known trapping potential.

A single atom exposed to resonant excitation light coherently oscillates with the single-atom Rabi frequency Ω_0 between the ground and excited state. An ensemble of N noninteracting atoms gives just N times the single-atom Rabi oscillation at frequency Ω_0. However, the ensemble of atoms can carry only one excitation if the interaction between two atoms in the excited state is much stronger than the linewidth of the excitation. As the excitation can be located at any of the N atoms this collective state is of the form

$$|\psi_e\rangle = \frac{1}{\sqrt{N}} \sum_{i=1}^{N} |g_1, g_2, g_3, \ldots, e_i, \ldots, g_N\rangle, \qquad (1)$$

where g_k indicates an atom numbered k in the ground state and e_i one atom i in the excited state. Therefore, the ensemble is excited collectively and oscillates with the collective Rabi frequency $\sqrt{N}\Omega_0$ between the ground state and the collective state ψ_e [13]. In this sense the ensemble of N atoms acts like a "superatom" [27] with a $\sqrt{N}$ larger transition matrix element.

The so-called "blockade radius" is defined as the interatomic distance at which the interaction energy equals the linewidth of the excitation, which is in our case dominated by power broadening due to the use of cw lasers and large detuning from the intermediate state [Fig. 1(a)]. In the simplest model, we estimate the blockade radius as the distance at which the van der Waals interaction C_6/r^6 equals the power-broadened linewidth $\hbar\Omega_0$ except for a geometric factor that includes the arrangement of superatoms:

$$r_b \propto [C_6/(\hbar\Omega_0)]^{1/6}. \qquad (2)$$

We define the strong blockade regime by a blockade radius being significantly larger than the mean interatomic distance, i.e., $N \gg 1$. In our experiments the sample size is larger than the blockade radius and we model the sample by an ensemble of superatoms. Additionally in our system, the density of ground state atoms is inhomogeneous and by this also the atom number per superatom N. Therefore the collective Rabi frequency is inhomogeneously distributed and the local oscillations add up to a total population that for short times increases quadratically. But after a very short time the Rydberg population shows a linear increase that falls behind the quadratic increase without interaction [see Fig. 1(b)]. This time is related to the inverse maximum collective Rabi frequency in the sample. For all experimental conditions shown in this Letter this time is shorter than 50 ns. For longer excitation times, the excitation in the strong blockade regime can be distinguished from single-atom behavior by a strong suppression of excitation [see the inset of Fig. 1(b)]. The time scale for the subsequent linear increase is proportional to the inverse of the aver-

aged collective Rabi frequency $\sqrt{N_{\mathrm{mean}}}\Omega_0$. Because of the inhomogeneity the excited state population saturates after a characteristic time, which is related to $(\sqrt{N_{\mathrm{mean}}}\Omega_0)^{-1}$. This population is determined by the number of superatoms in the sample. This number shows, as it will be explained below, a scaling with Ω_0 and the density of ground state atoms, which is characteristic for the underlying blockade mechanism.

Figure 2 shows the typical excitation dynamics for three different densities of the ground state atoms (a) and three different Rabi frequencies (b). Two features are prominent in the figure: an initial linear increase with time and a saturation to a constant number. In contrast to previous experiments at considerably lower densities, the dynamics should be described by full-quantum calculations [28] rather than a mean field model [4]. However, for the following investigations the excitation dynamics curves were fitted with a simple exponential saturation function of the form

$$N_R(\tau) = N_{\mathrm{sat}}(1 - e^{-R\tau/N_{\mathrm{sat}}}), \tag{3}$$

with the Rydberg atom number $N_R(\tau)$ after the excitation time τ, since we are mainly interested in the scaling of the saturation Rydberg atom number N_{sat} and the initial slope R. The inset in Fig. 2(a) contrasts the Rabi oscillation of noninteracting atoms with our measurement and demonstrates the strong blockade of excitation already in the early regime with linear increase.

Figure 3(a) shows the scaling of the initial slope R of the excitation with the density of ground state atoms. Assuming a constant blockade radius [see Eq. (2)], the averaged atom number $N_{\mathrm{mean}} = N_g/N_{\mathrm{sat}}$ per superatom is proportional to the peak density $n_{g,0}$ which was varied in the experiment. For noninteracting Rydberg atoms, the excited fraction would not depend on the number of atoms and R would scale linearly with $n_{g,0}$. In contrast, R shows a $\sqrt{n_{g,0}}$ scaling, which is clear evidence for a collective excitation. Furthermore, we investigated the scaling with the Rabi frequency Ω_0 by altering the intensity of the 780 nm laser. The initial excitation rate of noninteracting atoms or strongly damped (i.e., incoherent) excitation would scale with Ω_0^2. The linear scaling ($R \propto \Omega_0$) determined from Fig. 3(b) is evidence for coherent excitation of the Rydberg atoms. The combined $\sqrt{n_{g,0}}\Omega_0$ dependence is clear evidence for local coherent collective Rabi oscillations within a cloud of spatially inhomogeneous density.

As a further test of the predictions of the superatom model the scaling behavior of the saturation value N_{sat} was investigated. The saturation density of Rydberg atoms is proportional to r_b^{-3} and the saturation number of Rydberg atoms N_{sat} is proportional to their density. Thus from Eq. (2) N_{sat} is expected proportional to $\sqrt{\Omega_0}$ and independent of the ground state atom density. In reasonable agreement with this expectation we observe a very weak $n_{g,0}$ dependence in the saturation number of Rydberg atoms as shown in Fig. 4(a), although we change the ground state density by more than an order of magnitude.

The dependence of the saturation number of Rydberg atoms on the single-atom Rabi frequency as shown in Fig. 4(b) is close to the expected $\sqrt{\Omega_0}$ scaling, which is characteristic for van der Waals interaction. Note that additional N-dependent terms are expected in Eq. (2),

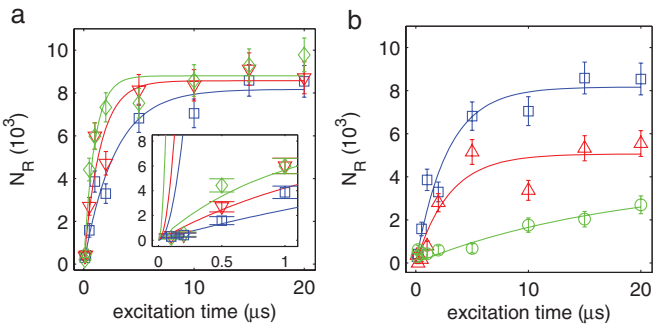

FIG. 2 (color). (a) The Rydberg atom number N_R plotted versus excitation time for a high laser intensity ($\Omega_0 =$ 210 kHz) and three values of the density of ground state atoms $n_{g,0} = [3.2 \times 10^{13}(\diamond),\ 6.6 \times 10^{12}(\triangledown),\ 2.8 \times 10^{12}(\square)]\ \mathrm{cm}^{-3}$. (b) The Rydberg atom number plotted versus excitation time for a low atom density ($n_{g,0} = 2.8 \times 10^{12}\ \mathrm{cm}^{-3}$) and three values of laser intensity $\Omega_0 = [210(\square),\ 93(\triangle),\ 42(\bigcirc)]$ kHz. The solid curves are fits to the data with a simple exponential saturation curve. The error bars represent the standard error of 5 measurements taken within one sample. The inset in (a) shows a magnification of the data in contrast with the calculated Rabi oscillations (three curves with faster increase) assuming negligible interactions.

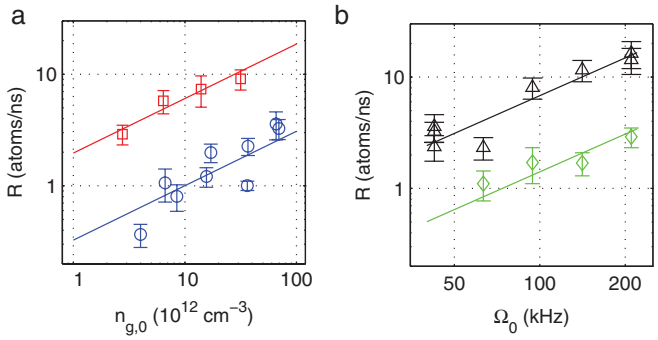

FIG. 3 (color). (a) Dependence of the initial increase R of the Rydberg atom number on the density of ground state atoms $n_{g,0}$ for high ($\square$) and low ($\bigcirc$) Rabi frequency $\Omega_0 = (210, 42)$ kHz. (b) Dependence of R on the excitation rate Ω_0 for high ($\triangle$) and low ($\diamond$) atom density $n_{g,0} = (7.2 \times 10^{13}, 2.8 \times 10^{12})\ \mathrm{cm}^{-3}$. The lines are power-law fits to the whole data set in (a) and (b) of the form $R \propto n_{g,0}^a \Omega_0^b$, which gives an exponent for the $n_{g,0}$ dependence of $a = 0.49 \pm 0.06$ which is in excellent agreement with the expected $\sqrt{n_{g,0}}$ scaling for collective excitation. The fitted exponent $b = 1.1 \pm 0.1$ for the Ω_0 scaling agrees well with $b = 1$ being expected for coherent excitation.

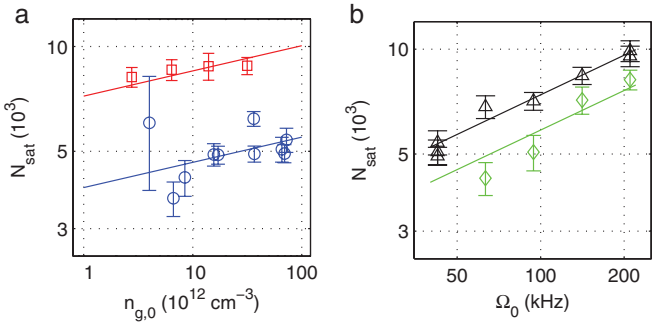

FIG. 4 (color). (a) Dependence of the saturation number of Rydberg atoms N_{sat} on the density of ground state atoms $n_{g,0}$ for high (□) and low (○) Rabi frequency $\Omega_0 = (210, 42)$ kHz. (b) Dependence of N_{sat} on the Rabi frequency Ω_0 for high (△) and low (◇) atom density $n_{g,0} = (7.2 \times 10^{13}, 2.8 \times 10^{12})$ cm^{-3}. The lines are the result of a power-law fit to the whole data set in (a) and (b) of the form $N_{\mathrm{sat}} \propto n_{g,0}^{c} \Omega_0^{d}$ which gives an exponent for the $n_{g,0}$ dependence of $c = 0.07 \pm 0.02$, which is in agreement with the expected independence from $n_{g,0}$ for strong blockade. The fitted exponent for the Ω_0 scaling is $d = 0.38 \pm 0.04$, which is in excellent agreement with the $\Omega_0^{2/5}$ scaling expected for a collective van der Waals blockade.

e.g., a $\sqrt{N}\Omega_0$ behavior of the collective Rabi frequency. With this refinement N_{sat} scales with $n_{g,0}^{1/5}\Omega_0^{2/5}$ improving the agreement with the measured Ω_0-dependence [Fig. 4(b)]. Other density dependent effects like the number of next neighbors that could explain the small deviation in the $n_{g,0}$ dependence are currently under further theoretical investigation.

The observation of the described scaling laws was enabled by working with dense samples. The average atom number per superatom N_{mean} was varied between 65 and 2500, while we expect N to be 1 order of magnitude higher in the center of the cloud. High atomic densities in the trapped cloud meant the collective Rabi frequency $\sqrt{N_{\mathrm{mean}}}\Omega_0$ was large compared to the laser linewidth; this allowed the observation of the characteristic scalings with Ω_0.

To conclude, we have found evidence for mesoscopic quantum dynamics of frozen Rydberg gases in the strong blockade regime. Mesoscopic size effects on the coherent evolution have been identified for up to a few thousand atoms per mesoscopic unit. This became possible by narrowband excitation of magnetically trapped atoms at temperatures of a few microkelvin and variable densities. Analogous size effects are expected in other mesoscopic systems carrying a single quantum of excitation only. The demonstrated scalability of the system will enable studies of size dependent quantum correlations and decoherence effects in strongly interacting nonequilibrium situations.

We would like to thank H. Bender who set up the GHz source and T. Lahaye for proofreading. We acknowledge financial support from the DFG within No. SFB/TRR21, No. SFB407, No. SPP116, and under Contract No. PF 381/4-1, U. K. acknowledges support from the Landesgraduiertenförderung Baden-Württemberg.

*r.heidemann@physik.uni-stuttgart.de
†t.pfau@physik.uni-stuttgart.de

[1] J. Raimond, G. Vitrant, and S. Haroche, J. Phys. B **14**, L655 (1981).
[2] I. Mourachko *et al.*, Phys. Rev. Lett. **80**, 253 (1998).
[3] W. R. Anderson, J. R. Veale, and T. F. Gallagher, Phys. Rev. Lett. **80**, 249 (1998).
[4] D. Tong *et al.*, Phys. Rev. Lett. **93**, 063001 (2004).
[5] K. Singer *et al.*, Phys. Rev. Lett. **93**, 163001 (2004).
[6] T. Cubel Liebisch, A. Reinhard, P. R. Berman, and G. Raithel, Phys. Rev. Lett. **95**, 253002 (2005).
[7] T. Cubel *et al.*, Phys. Rev. A **72**, 023405 (2005).
[8] T. Vogt *et al.*, Phys. Rev. Lett. **97**, 083003 (2006).
[9] K. Afrousheh *et al.*, Phys. Rev. A **73**, 063403 (2006).
[10] T. J. Carroll, S. Sunder, and M. W. Noel, Phys. Rev. A **73**, 032725 (2006).
[11] J. Deiglmayr *et al.*, Opt. Commun. **264**, 293 (2006).
[12] D. Jaksch *et al.*, Phys. Rev. Lett. **85**, 2208 (2000).
[13] M. D. Lukin *et al.*, Phys. Rev. Lett. **87**, 037901 (2001).
[14] A. K. Mohapatra, T. R. Jackson, and C. S. Adams, Phys. Rev. Lett. **98**, 113003 (2007).
[15] M. Fleischhauer, A. Imamoglu, and J. P. Marangos, Rev. Mod. Phys. **77**, 633 (2005).
[16] L.-M. Duan, M. D. Lukin, J. I. Cirac, and P. Zoller, Nature (London) **414**, 413 (2001).
[17] Y. Colombe *et al.*, arXiv:0706.1390.
[18] R. Loew *et al.*, arXiv:0706.2639.
[19] W. Li, P. J. Tanner, and T. F. Gallagher, Phys. Rev. Lett. **94**, 173001 (2005).
[20] A. Grabowski *et al.*, Fortschr. Phys. **54**, 765 (2006).
[21] U. Raitzsch *et al.*, arXiv:0706.3869 (to be published).
[22] T. F. Gallagher, *Rydberg Atoms* (Cambridge University Press, Cambridge, U.K., 1994).
[23] B. Knuffman and G. Raithel, Phys. Rev. A **73**, 020704(R) (2006).
[24] K. Singer, J. Stanojevic, M. Weidemüller, and R. Côté, J. Phys. B **38**, S295 (2005).
[25] W. Li *et al.*, Phys. Rev. A **70**, 042713 (2004).
[26] M. P. Robinson *et al.*, Phys. Rev. Lett. **85**, 4466 (2000).
[27] V. Vuletic, Nature Phys. **2**, 801 (2006).
[28] F. Robicheaux and J. V. Hernández, Phys. Rev. A **72**, 063403 (2005).